

Journal of Biomedical Optics

BiomedicalOptics.SPIEDigitalLibrary.org

Table top surface plasmon resonance measurement system for efficient urea biosensing using ZnO thin film matrix

Ayushi Paliwal
Monika Tomar
Vinay Gupta

SPIE.

Ayushi Paliwal, Monika Tomar, Vinay Gupta, "Table top surface plasmon resonance measurement system for efficient urea biosensing using ZnO thin film matrix," *J. Biomed. Opt.* **21**(8), 087006 (2016), doi: 10.1117/1.JBO.21.8.087006.

Table top surface plasmon resonance measurement system for efficient urea biosensing using ZnO thin film matrix

Ayushi Paliwal,^a Monika Tomar,^b and Vinay Gupta^{a,*}

^aUniversity of Delhi, Department of Physics and Astrophysics, Delhi 110007, India

^bUniversity of Delhi, Physics Department, Miranda House, Delhi 110007, India

Abstract. The present report addresses the application of surface plasmon resonance (SPR) phenomenon for urea sensing. The former promises a high sensitivity, label-free detection, and real-time information by monitoring the refractive index change at the metal–dielectric interface. In the present report, a highly sensitive urea biosensor has been developed by integrating a ZnO thin film matrix with the SPR technique. Kretschmann configuration has been used to excite the surface plasmon (SP) modes at the ZnO–metal (gold) interface using an indigenously developed table top SPR measurement setup. Urease (Urs), the urea-specific enzyme, has been immobilized on the surface of ZnO thin film by physical adsorption technique. The SPR reflectance curves were recorded for the prism/Au/ZnO/Urs system in angular interrogation mode with phosphate-buffered saline (PBS) solution as the liquid media. The SPR resonance angle is found to be shifted toward a lower angle from 49.1 to 42.0 deg with an increase in the urea concentration (0 to 300 mg/dl) in the PBS solution. The developed sensor (prism/Au/ZnO/Urs) is found to be highly sensitive [sensitivity = 0.039 deg/(mg/dl) or 203 deg/RIU] with detection accuracy of 0.045(deg)⁻¹. © 2016 Society of Photo-Optical Instrumentation Engineers (SPIE) [DOI: 10.1117/1.JBO.21.8.087006]

Keywords: surface plasmon resonance; immobilization; bio-molecule; refractive index; extinction coefficient.

Paper 160292R received May 11, 2016; accepted for publication Aug. 2, 2016; published online Aug. 23, 2016.

1 Introduction

The last few decades have witnessed a surge in the demand for fast, sensitive, and easy-to-use biosensors primarily for biomedical applications. Optical biosensors exhibit many advantages over other conventional biosensing technologies, including resistance to chemically reactive ambience, high immunity toward electromagnetic (EM) interference, and so on. Among all the available optical detection techniques, surface plasmon resonance (SPR) is one of the most efficient techniques for biomolecular interaction analysis due to its high sensitivity, label-free detection, and ability for real-time measurements.^{1–3}

Surface plasmons (SPs) can be considered as the surface bound EM modes arising due to the resonant coupling of optical EM waves with the free electrons of a metal. The SP modes are excited typically at the interface of metal and dielectric, where the two adjacent materials have opposite dielectric constants. The field intensity of SPs is maximum at the metal–dielectric interface while an evanescent wave which is used to excite the SPs decays exponentially into both the adjacent media. The excitation of SPs by the evanescent wave is achieved when the evanescent wave propagation constant becomes equal to the SP wave propagation constant, also known as the resonance condition. At resonance angle, the energy carried by the photons (evanescent wave) is transferred to the SPs, due to which the intensity of the reflected light becomes negligible. The resonance angle is highly sensitive to the material properties, specifically the refractive index of the metal and dielectric.

Refractometric sensing platforms are based on this unique property exhibited by SPs, where a change in refractive index in the vicinity of metal–dielectric interface (due to the attachment or recognition of biomolecule) alters the excitation or dispersion relation of SPs. Hence, SPR biosensors provide a promising platform for the detection of various biomolecular interactions,⁴ including DNA- and RNA hybridization,^{5–7} antibody–antigen interaction,^{8–10} enzymatic reactions,¹¹ and so on.

Urea, an end product of the nitrogen metabolism, is an important entity in human blood for the proper functioning of liver and kidney. Any variation or change in the urea concentration from normal level (10 to 20 mg/dl) can lead to viabl-nephritic syndrome, hepatic failure, cachexia, dehydration, shock, urinary tract obstruction, gastrointestinal bleeding, and so on.^{12,13} Thus, the identification of urea above the normal concentration is very important for control and diagnosis of related diseases. Though there are reports on detection of urea using other detection techniques, limited work has been done using SPR technique. Verma and Gupta¹⁴ reported the detection of urea and glucose using SPR biosensor based on optical fiber coupling, however, the selectivity of the fabricated biosensor is not studied. Moreover, optical fiber coupling is not a viable method for practical applications. The deposition of metal film on the core surface of an optical fiber demands precision and uniformity and also it is very difficult to launch light into optical fiber coupler, whereas prism-based geometry for the excitation of SPs is advantageous as it is slightly easier for metallic deposition and provides good surface area for functionalization of the sensing surface.

*Address all correspondence to: Vinay Gupta, E-mail: drvguptavinay@gmail.com, vgupta@physics.du.ac.in

For the realization of a biosensor, a biorecognition element is foremost required and in that regime, metal oxides are reported to be efficient. Zinc oxide (ZnO) is a biocompatible material which has emerged as a suitable matrix for immobilization of biomolecules due to its unique material properties.^{15,16} Thus, ZnO has been chosen as a suitable matrix in the present work for immobilization of urea-specific enzyme (Urease, Ur). A prism/Au/AnO/Ur biosensor has been utilized for the detection of urea in phosphate-buffered saline (PBS) buffer (0 to 300 mg/dl) in static and dynamic modes. An indigenously developed SPR measurement setup has been utilized for the study. Selectivity of the fabricated bioelectrode has been tested in the presence of other interfering biomolecules in the solution.

2 Experimental Details

2.1 Materials

Urs (Source: Jack Beans) was purchased from Sigma-Aldrich (Catalog number: 9002-13-5). Urea was used as an analyte in the present work, which was procured from Sisco Chemicals, India (Catalog number: 57-13-6). For preparing buffer solution, sodium phosphate monobasic anhydrous and sodium phosphate dibasic dihydrate were procured from Sisco Chemicals, India.

2.2 Preparation of Solutions

Deionized water (DI; resistivity = $18.2 \text{ M}\Omega\text{cm}^{-1}$) was used as a solvent to prepare the aqueous solutions. PBS 50 mM, pH 7.0 (0.9% NaCl) solution was prepared by adjusting the proportion of 0.2 M monobasic sodium phosphate solution with 0.2 M dibasic sodium phosphate solution and subsequently adding 0.9% NaCl to the solution. Urs enzyme solution (1 mg/ml) was prepared in a fresh PBS buffer solution maintained at a pH of 7.0. The urea concentration varying from 0 to 300 mg/dl was prepared in fresh DI.

2.3 Preparation of the Sensor and Immobilization of Urease

To fabricate the prism-based SPR sensor, a gold (Au) thin film of optimized thickness (40 nm) is deposited directly on the largest face (hypotenuse face) of the glass prism (BK-7) using thermal evaporation technique at a base pressure of 10^{-6} mbar. The thickness of the Au film is controlled via quartz crystal thickness monitor. The Au-coated prisms are then post-annealed in air at 250°C for 1 h to attain a stable SPR response and improve its adhesion. radio frequency (RF)-magnetron sputtering technique is used for depositing a ZnO thin film (sensing layer) of 200 nm thickness on Au-coated prisms. The deposition parameters of ZnO thin film are taken from our previously reported work.¹⁷ ZnO thin film of the same thickness was also deposited on glass substrates under similar deposition conditions for the structural and morphological characterization. Subsequently, a low isoelectric point, IEP (5.1), $10 \mu\text{l}$ solution of Ur enzyme (1.0 mg/ml) prepared in phosphate buffer is immobilized carefully on ZnO thin film coated prism/Au surface by physical adsorption technique. High IEP of ZnO (8.7 to 10.3) supports the strong electrostatic interaction between the enzyme (Ur) and the ZnO surface. After enzyme immobilization, the prisms are washed thoroughly with DI water to remove unbound enzyme molecules and stored at 4°C .

2.4 Measurement and Surface Plasmon Resonance Experimental Setup

The structural and crystallographic studies of deposited ZnO thin film have been carried out using a Bruker D 80 x-ray diffractometer. The surface morphology of the sensor surface, i.e., ZnO thin film deposited on Au-coated glass substrate and the Ur biomolecule immobilized on its surface was explored with Atomic Force Microscope (AFM; Bruker Dimension Icon). In the present work, an indigenously developed SPR measurement setup based on Kretschmann configuration is used to excite the SP modes at the interface of Au and ZnO. A schematic of the prism-based SPR urea sensor is shown in Fig. 1. A detailed description of the indigenously developed SPR setup is explained in our earlier work.¹⁸ A separate liquid sample cell of glass is developed, which is attached to the Ur/ZnO/Au coated prism such that the hypotenuse face of the prism, where Au and ZnO thin films are deposited, is in direct contact with the different concentrations of urea solution (analyte) varying from 0 to 300 mg/dl (Fig. 1). The SPR curves for the prism/Au/ZnO/biomolecules/buffer system were recorded in angular interrogation mode by inserting different concentrations of urea solution in the PBS buffer kept in contact with the sensor (prism/Au/ZnO/Ur) surface (static mode) and the corresponding resonance angles are noted. The change in reflectance with increase in the concentration of urea solution at fixed resonance angle is measured with time using a CCD camera (dynamic mode).

3 Results and Discussion

3.1 Structural and Morphological Properties of Sputtered ZnO Thin Film

The XRD pattern of ZnO thin film deposited over a glass substrate is shown in Fig. 2(a). There exists only a single peak corresponding to (002) plane of the wurtzite structure of ZnO at $2\theta \sim 34.25^\circ$ deg confirming the deposition of a *c*-axis oriented ZnO thin film by the RF sputtering technique.¹⁹ The value of crystallite size was estimated to be 23 nm using Scherrer's equation.²⁰

The AFM image of the ZnO thin film grown on glass substrate is shown in Fig. 2(b). The surface morphology of ZnO thin film was smooth having uniformly distributed nanosize crystallites along with nanopores. Significant variation in the surface morphology was observed in the AFM images [Fig. 2(c)] of ZnO thin film after immobilization of Ur enzyme. Globular structures of about $1.5 \mu\text{m}$ diameter could be observed in the AFM image confirming the successful immobilization of Ur on the surface of ZnO thin film.¹⁷

3.2 Surface Plasmon Resonance Studies

3.2.1 Optimization of the thickness of Au and ZnO thin films for sharp surface plasmon resonance reflectance curve

The theoretical simulations have been performed for optimizing the Au film thickness. Figures 3(a) and 3(b) show the theoretical simulation results for prism/Au/air configuration by varying the thickness of Au thin film from 10 to 100 nm.

The values of reflectance at metal-dielectric (air) interface were estimated theoretically using the Fresnel's equation by varying the angle of incidence of light (angular interrogation

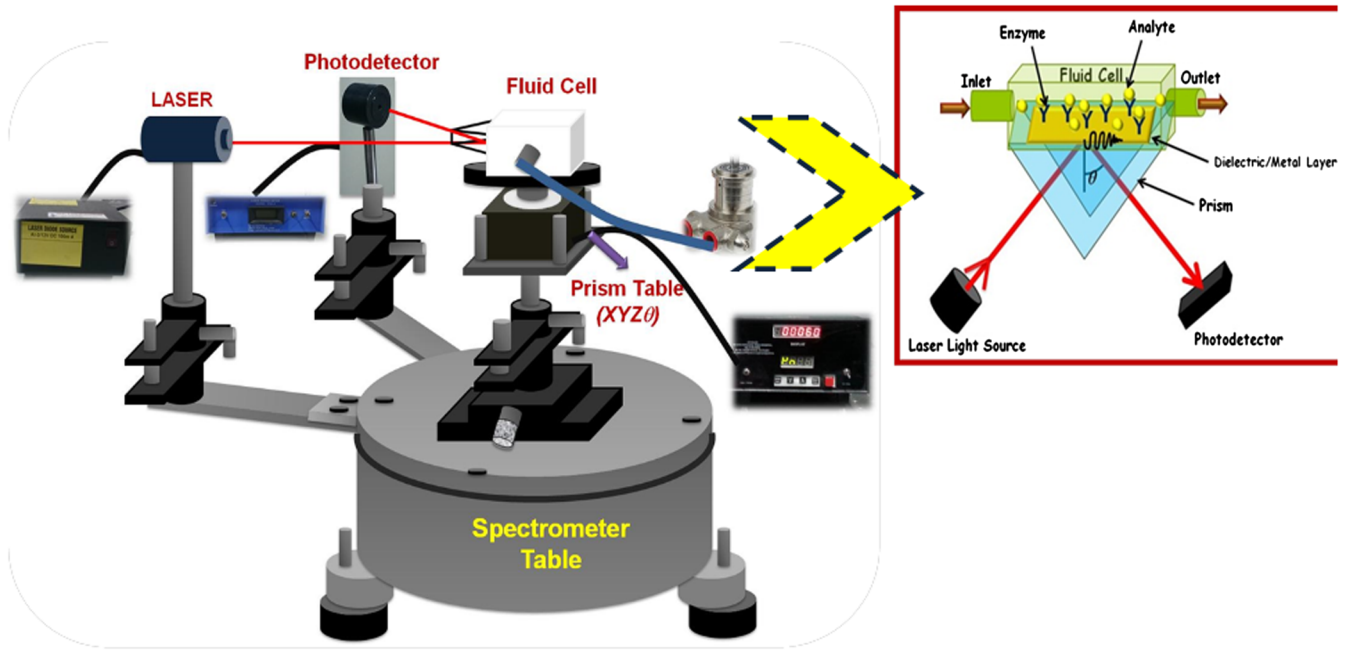


Fig. 1 Schematic of the prism-based SPR urea sensor using prism/Au/ZnO system.

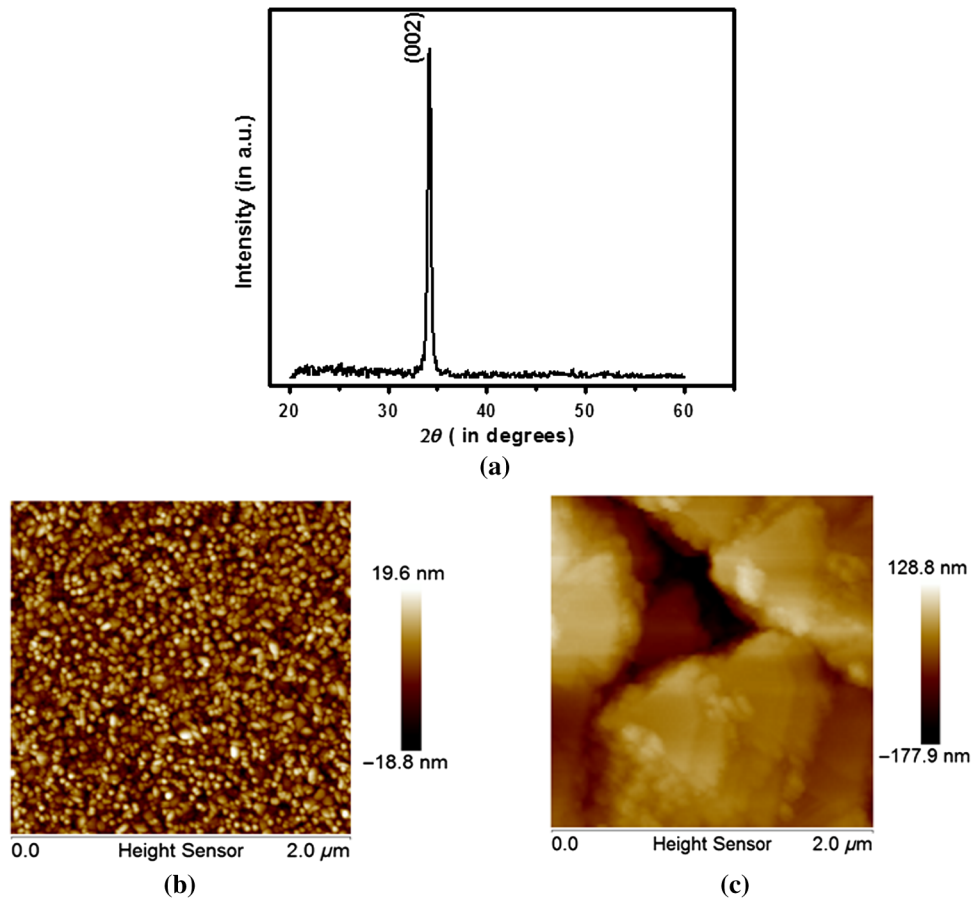


Fig. 2 (a) XRD spectra of RF-magnetron sputtered ZnO thin film, (b) AFM image of ZnO/Au bilayer, and (c) AFM image of Ur enzyme immobilized over ZnO/Au bilayer.

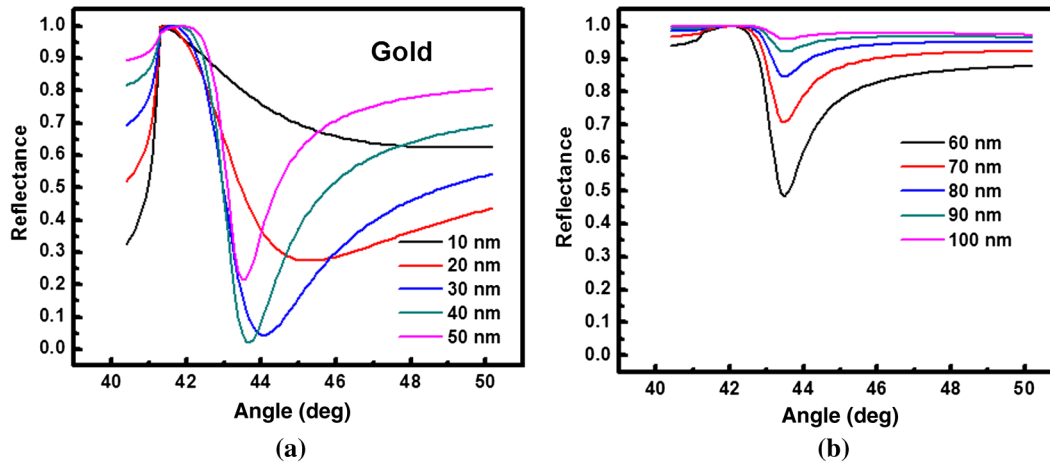


Fig. 3 (a) Theoretically simulated SPR reflectance curves for metal/air interface for varying thickness 10 to 50 nm of gold film and (b) theoretically simulated SPR reflectance curves for varying thickness from 50 to 100 nm.

from 40 to 50 deg).¹⁸ The values of thickness are decided by taking into account the reported values of the dielectric constant of Au metal.²¹ For more clarity, the variation in SPR curves is shown in two thickness ranges separately, i.e., 0 to 50 nm and 60 to 100 nm. As is evident from Fig. 3(a), the value of reflectance and broadness of the SPR reflectance curve is continuously decreasing with an increase in thickness of the Au film from 10 to 40 nm. Moreover, on increasing the thickness (>40 nm) of the Au layer further, the reflectance is found to be increasing. Thus, a 40-nm thin Au film exhibits the best SPR curve with minimum losses and shows the sharpest SPR dip. It is also noted from Figs. 3(a) and 3(b) that the resonance dip angle (θ_{SPR}), where reflectance is minimum (R_{min}), shifts toward a lower angle with increasing thickness of the Au thin film. In general, the SPR curves for the metal–air interface can be divided into two categories (1) lower range, where the sharpness of the curve increases along with a decrease in value of R_{min} with the thickness of the metal film and (2) higher thickness range, where the sharpness of the curve decreases along with an increase in the value of R_{min} with the thickness of the metal layer. The results may be related to the fact that at very low thickness of metal film, the electron density is not

sufficient enough to absorb the incident laser energy due to which less reflectance minima along with a broader reflectance curve is observed. On the other hand, for a higher thickness of the metal film, the losses in the metal film degrade the SPR reflectance curves resulting in a higher value of reflectance minima and FWHM.

The thickness of the ZnO thin film for prism/Au/ZnO/air configuration has also been optimized experimentally by varying its thickness from 50 to 300 nm. The SPR reflectance curves for prism/Au/ZnO/air configuration by varying thickness of ZnO are given in Fig. 4.

As is evident from Fig. 4, the SPR reflectance curve for a 200-nm thick ZnO thin film in prism/Au/ZnO/air configuration gives the sharpest SPR curve. Thus, the 200-nm thick ZnO film has been utilized for sensing applications.

Hence, the system prism/Au/ZnO/air having an Au thickness of 40 nm and ZnO thickness of 200 nm was optimized used for further biosensing applications.

3.2.2 Surface plasmon resonance reflectance curve for prism/Au/buffer, prism/Au/ZnO/buffer and prism/Au/ZnO/Ur/buffer systems using angular interrogation method

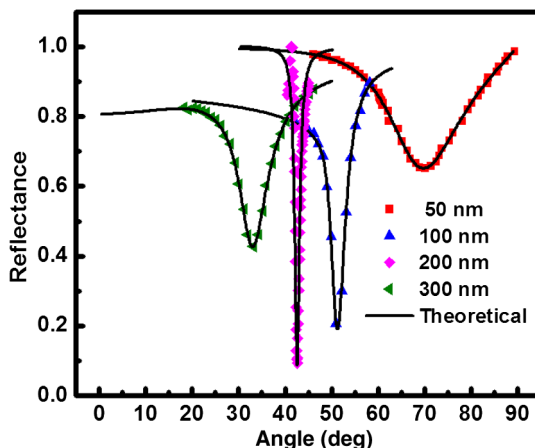


Fig. 4 SPR reflectance curves obtained for the prism/Au/ZnO/air system for varying thickness of ZnO thin film.

The SPR studies for all the systems were performed in PBS buffer solution so as to prevent the denaturation of Urs enzyme immobilized over prism/Au/ZnO. In the present case, PBS buffer is taken as the semi-infinite media instead of air. The SPR reflectance curve for prism/Au/buffer at $\lambda = 633$ nm is shown in Fig. 5, where the optimized thin film of 40 nm Au is used to excite the SP mode at the metal–PBS interface. The minimum reflectance is observed to be $R_{\text{min}} \sim 0.18$ at an incident angle $\theta_{\text{SPR}} \sim 43.1$ deg (Fig. 5) related to the SP wave excited at the interface of Au–PBS buffer. The observed SPR curve for prism/Au/buffer is found to be similar to the SPR curve reported by other workers for prism/Au/air.¹⁹ The FWHM of the SPR reflectance curve increases (i.e., SPR curve becomes broad) and the SPR resonance angle shifts to a higher angle (48.4 deg) after depositing the ZnO thin film on Au coated glass prisms, as shown in Fig. 5. The SPR curves shown in Fig. 5 were fitted to Fresnel's equations to determine the dielectric constant and refractive index of the film.²² The

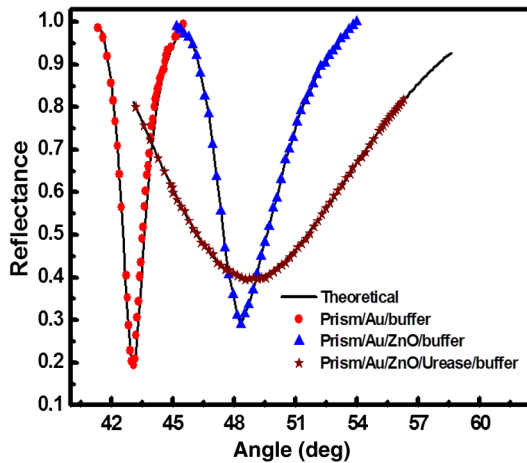


Fig. 5 SPR reflectance curves obtained for the prism/Au/buffer, prism/Au/ZnO/buffer, and prism/Au/ZnO/Urs/buffer systems.

complex dielectric constant ($4.884 + 0.01i$) and refractive index ($2.210 + 0.0023i$) for ZnO film were found to match well with the reported values.¹⁹ The well-defined SPR reflectance curve was obtained for the prism/Au/ZnO/Urs/buffer system at $\lambda = 633$ nm, as shown in Fig. 5. Here, the FWHM of SPR reflectance curve becomes much larger and θ_{SPR} shifts to a higher angle (i.e., $\theta_{SPR} \sim 48.9$ deg) as compared to prism/Au/buffer and prism/Au/ZnO/buffer systems (Fig. 5). The complex dielectric constant of the biomolecule (i.e., Urs) was determined using Fresnel's equations²³ and matches well to the reported value.¹⁸

3.2.3 Response characteristics of urea biosensor using surface plasmon resonance

Surface plasmon resonance reflectance curves for prism/Au/ZnO/Urs/buffer system. To study the application of SPR in urea sensing, the SPR reflectance curves were recorded in angular interrogation mode for prism/Au/ZnO/Urs/buffer system for varying concentrations of urea (0 to 300 mg/dl) in PBS buffer solution separately, as depicted in Fig. 6(a). It is

clearly seen that the SPR resonance angle, θ_{SPR} , continuously decreases linearly from 49.1 to 43.0 deg with the increase in the urea concentration from 0 to 200 mg/dl in the buffer solution [Fig. 6(b)] and is due to the hydrolysis of urea catalyzed by the enzyme Ur. But increasing the concentration from 200 to 300 mg/dl, the variation of SPR resonance angle, θ_{SPR} , gets saturated, which suggests the saturation of active sites of the enzymes at this urea level.

Sensing mechanism. The Ur enzyme immobilized on the ZnO/Au bilayer acts as a catalyst for the hydrolysis of urea, leading to the formation of bicarbonate, ammonium, and hydroxide ions governed by the following reaction:^{24,25}



In the prism-based SPR sensor, the decrease in the resonance angle (θ_{SPR}) is due to the decrease in the refractive index of the sensing medium in contact with the sensing layer (i.e., ZnO).^{26,27} Thus, a decrease in the refractive index of the immobilized layer of the enzyme (i.e., Urs) due to the formation of the complex between enzyme (Ur) and analyte (urea) leads to the decrease in resonance angle. The refractive index of the products of the enzymatic reactions, i.e., ammonium ions and bicarbonate ions is less than the effective refractive index of the ZnO layer over which Ur enzyme is immobilized (around 2.21).^{19,28,29} Thus, the effective refractive index of the sensing media decreases due to the reaction between Ur enzyme and analyte urea. Now, as the concentration of urea solution increases in the sample cell, there is a consequent decrease in the refractive index of the sensing medium leading to a continuous decrease in the resonance angle with an increase in the concentration of the analyte (urea).

Sensitivity and detection accuracy. It may be noted from Fig. 6(b) that the variation in θ_{SPR} with urea concentration is linear. The error bars take into account the measurement accuracies by each component of the experimental setup. The sensitivity of the prepared sensor was calculated by taking the ratio of change in the resonance angle with the increase in urea concentration. The sensitivity of SPR biosensor has been estimated

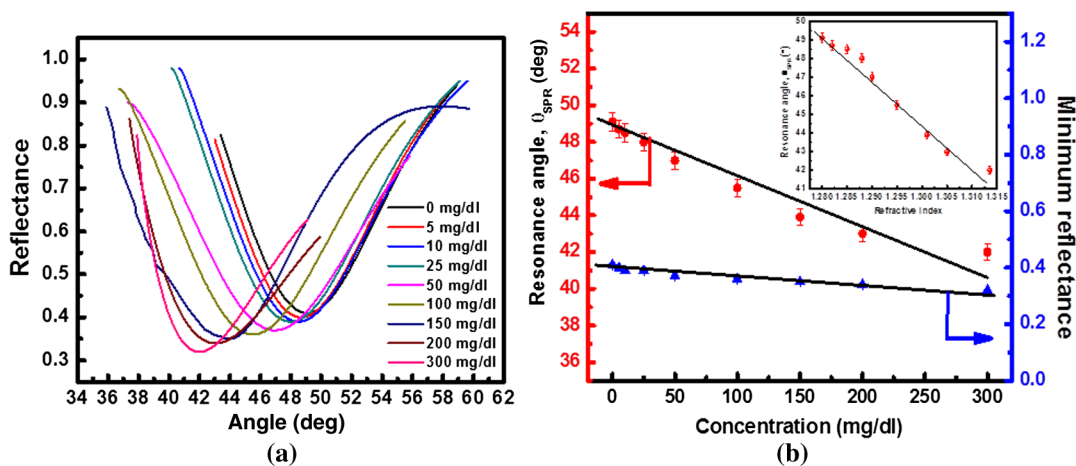


Fig. 6 (a) SPR reflectance curves for prism/Au/ZnO/Urs/buffer system for increasing concentration of urea from 0 to 300 mg/dl and (b) variation of resonance angle (θ_{SPR}) and minimum reflectance with the concentration of Urs.

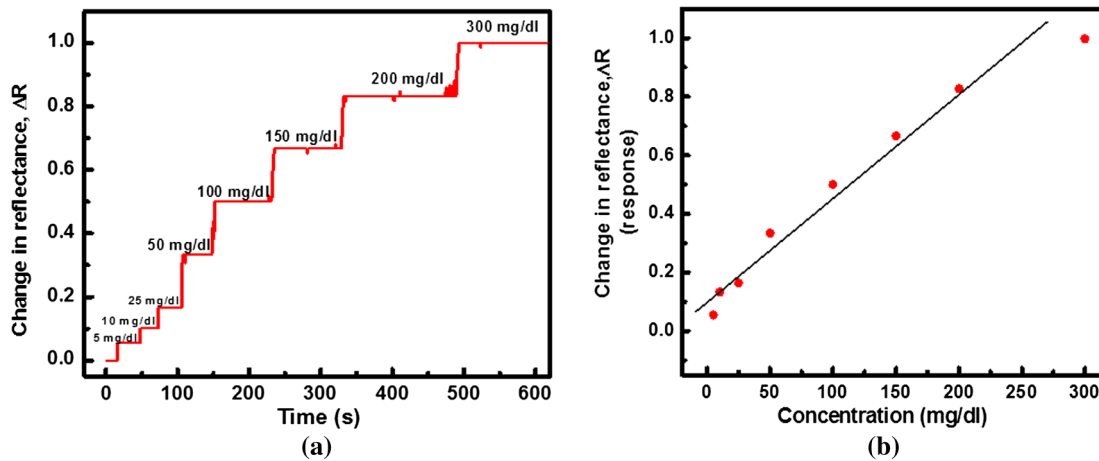


Fig. 7 (a) Dynamic variation of change in sensor response with increase in urea concentration from 0 to 300 mg/dl and (b) the calibration curve of the sensor, i.e., the variation of change in reflectance with increase in concentration from 0 to 300 mg/dl.

to be about $0.039 \text{ deg}/(\text{mg}/\text{dl})$. Sensitivity can also be defined in terms of the shift in resonance angle per unit change in the refractive index of the sensing medium. Hence, the variation in resonance angle is again plotted with the refractive index and is shown in the inset of Fig. 6(b). The sensitivity of the prepared sensor was recalculated by taking the ratio of change in the resonance angle with the increase in the refractive index of the sensing medium. The sensitivity of the SPR biosensor has been estimated to be about $203 \text{ deg}/\text{RIU}$. The detection accuracy is the inverse of the spectral width of the SPR curves obtained experimentally for different concentrations of urea. Hence, the detection accuracy of the prepared urea biosensor prism/Au/ZnO/Urs/buffer toward urea is estimated to be about $0.045(\text{deg})^{-1}$. Figure of merit (FOM) has been estimated for a SPR-based biosensor. FOM is defined as the ratio of sensitivity and full width at half maximum (FWHM) of the SPR reflectance curve. In the present work, FWHM of all SPR reflectance curves has been evaluated and was found to be almost same. Thus, FOM was found by taking the ratio of sensitivity and FWHM values of the prepared biosensor. FOM of the prepared sensor having a particular sensitivity and FWHM of the SPR reflectance curve was calculated to be $0.0037 (\text{mg}/\text{dl})^{-1} (20.1 \text{ RIU}^{-1})$.

Koncki et al.³⁰ have designed an enzyme-based biosensor based on pH bulk optode membrane that suffers from the shortcoming of low sensitivity and interference. Ansari et al.³¹ have developed an electrochemical urea sensor using sol-gel derived CeO_2 film having a sensitivity of $0.64 \mu\text{A}/\text{mg}/\text{dL}$. Stasyuk et al.³² have designed a novel urea biosensor based on polyaniline–nafion composite using amperometric technique and obtained a sensitivity of $110 \text{ nA}/\text{mM mm}^2$, which is very low in comparison to the sensitivity of the sensor obtained in the present work ($203 \text{ deg}/\text{RIU}$). There are some disadvantages of amperometric enzyme-based biosensors over the optical ones, such as interference from chemicals present in the sample matrix and it is especially problematic in biological samples in particular, as there are often electrochemical interferences in the sample matrix.

Dynamic response of the surface plasmon resonance sensor. For measuring the transient response of the SPR urea biosensor, the angle of incidence is fixed at the SPR dip

angle, $\theta_{\text{SPR}} = 49.1 \text{ deg}$. Subsequently, the change in reflectance of the SPR biosensor is monitored using a CCD camera for a particular concentration of urea in PBS solution (without urea). Figure 7(a) shows the transient response (change in reflectance; ΔR) of the SPR biosensor. It is clear from Fig. 7(a) that response (ΔR) increases continuously with an increase in the urea concentration from 0 to 300 mg/dl, which is mainly due to the interaction of the biorecognition enzyme (Ur) with the analyte (urea). The observed variation in ΔR with urea concentration is due to change in the refractive index of the bulk media and the sensing layer. The sensing response of the SPR biosensor increases gradually with the increase in urea concentration due to the rise in the attachment of the urea (analyte) onto active sites of immobilized Ur on the surface of the prism/Au/ZnO structure. For quantification of analyte (urea), the sensing response (ΔR) of SPR biosensor prism/Au/ZnO/Urs/buffer was plotted as a function of urea concentration and the calibration curve is shown in Fig. 7(b). The response was found to increase linearly from 0.055 to 0.827 with the increase in urea concentration from 5 to 200 mg/dl [Fig. 7(b)] and again showed a saturation by increasing the concentration to 300 mg/dl.

The presently prepared biosensor based on SPR is linear over a wide range of analyte concentration, up to 200 mg/dl. The results obtained with the SPR biosensor in the present study are encouraging and indicative of the availability of a large number of active sites on the surface of the SPR probe, which results in an enhanced response over a wide linear range of analyte concentration with stability.

Selectivity and reusability of the biosensor. In order to study the selectivity of prism/Au/ZnO/Urs bioelectrode toward the detection of urea, SPR measurements have been carried out by adding a normal concentration of the possible interferents present in human serum, such as glucose (5.0 mM), uric acid (0.1 mM), cholesterol (5.0 mM), and sodium content (140 mM), separately along with a normal concentration of urea (1 mM), as shown below in Figs. 8(a)–8(d). No significant shift was observed in the SPR curves. The measurements were repeated five times and the relative standard deviation was found to be less than 2%. The sensor, thus, displays high selectivity toward urea.

The prism/Au/ZnO/Urs biosensor was found to be reusable and suitable for practical applications. The prism/Au/ZnO/Urs

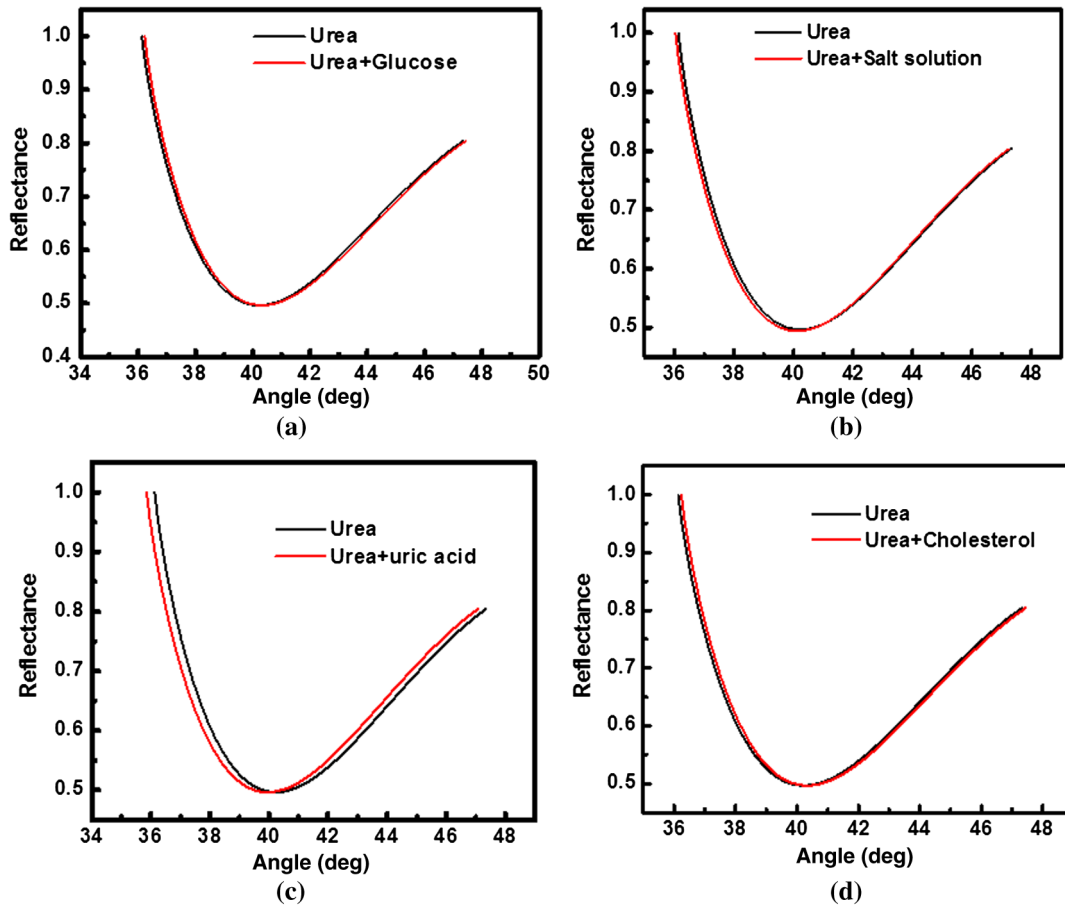


Fig. 8 Effect of various interferents on prism/Au/ZnO/Urs biosensor: (a) SPR reflectance curves after the addition of urea and urea + glucose solution, (b) SPR reflectance curves after the addition of urea and urea + salt (or sodium) solution, (c) SPR reflectance curves after the addition of urea and urea + uric acid solution, and (d) SPR reflectance curves after the addition of urea and urea + cholesterol solution.

biosensor was regenerated after every measurement. The SPR measurements were repeated three times for a particular concentration of analyte. For all the concentration of analyte chosen in the present work, the biosensor was regenerated 21 times and was found to give the same base line. This indicates the proper regeneration of the biosensor and its reusability. The error in the repeated cycles for a particular analyte concentration was found to be around 5% for the entire range of concentration of the analyte.

4 Conclusion

A prism-based SPR sensor for urea detection using the SPR technique has been fabricated and characterized. The principle of the detection of urea is based on the enzymatic reaction between Ur and the urea solution. The sensor comprises of four layers, namely, prism, gold, ZnO, and enzyme (Urs). The ZnO thin film is used to immobilize Ur on its surface by the physical adsorption technique. The SPR reflectance curves were recorded in angular interrogation mode for increasing concentration of urea solution using a p-polarized He-Ne laser beam at 633-nm wavelength. The fabricated SPR biosensor prism/Au/ZnO/Urs/buffer shows a continuous decrease in the SPR reflectance angle with an increase in the concentration of the analyte (urea). The sensor shows a high sensitivity [0.039 deg/(mg/dl)], reusability, and reproducibility for urea detection making it appropriate for practical applications.

Acknowledgments

Authors are thankful to Department of Science and Technology, India, for financial support.

References

1. B. Liedberg, C. Nylander, and I. Lundstrom, "Biosensing with surface plasmon resonance—how it all started," *Biosens. Bioelectron.* **10**, i–ix (1995).
2. B. K. Oh et al., "Surface plasmon resonance immunosensor for the detection of Salmonella typhimurium," *Biosens. Bioelectron.* **19**, 1497–1504 (2004).
3. X. D. Hoa, A. G. Kirk, and M. Tabrizian, "Towards integrated and sensitive surface plasmon resonance biosensors: a review of recent progress," *Biosens. Bioelectron.* **23**, 151–160 (2007).
4. J. Homola, "Surface plasmon resonance sensors for detection of chemical and biological species," *Chem. Rev.* **108**, 462–493 (2008).
5. A. J. Thiel et al., "In situ surface plasmon resonance imaging detection of DNA hybridization to oligonucleotide arrays on gold surfaces," *Anal. Chem.* **69**, 4948–4956 (1997).
6. L. He et al., "Colloidal Au-enhanced surface plasmon resonance for ultrasensitive detection of DNA hybridization," *J. Am. Chem. Soc.* **122**, 9071–9077 (2000).
7. A. Iguchi et al., "RNA binding properties of novel gene silencing pyrrole-imidazole polyamides," *Biol. Pharm. Bull.* **36**, 1152–1158 (2013).
8. M. Malmqvist, "Surface plasmon resonance for detection and measurement of antibody-antigen affinity and kinetics," *Curr. Opin. Immunol.* **5**, 282–286 (1993).

9. R. Karlsson and A. Falt, "Experimental design for kinetic analysis of protein-protein interactions with surface plasmon resonance biosensors," *J. Immunol. Methods* **200**, 121–133 (1997).
10. D. K. Weeraratne et al., "Development of a biosensor-based immunogenicity assay capable of blocking soluble drug target interference," *J. Immunol. Methods* **396**, 44–55 (2013).
11. Y. Iwasaki, T. Horiuchi, and O. Niwa, "Detection of electrochemical enzymatic reactions by surface plasmon resonance measurement," *Anal. Chem.* **73**, 1595–1598 (2001).
12. V. Bisht, W. Takashima, and K. Kaneto, "An amperometric urea biosensor based on covalent immobilization of urease onto an electrochemically prepared copolymer poly (N-3-aminopropyl pyrrole-copolyrrole) film," *Biomaterials* **26**, 3683–3690 (2005).
13. G. Dhawan, G. Sumana, and B. D. Malhotra, "Recent developments in urea biosensors," *Biochem. Eng. J.* **44**, 42–52 (2009).
14. R. Verma and B. D. Gupta, "A novel approach for simultaneous sensing of urea and glucose by SPR based optical fiber multianalyte sensor," *Analyst* **139**, 1449–1455 (2014).
15. A. Ali et al., "Nanostructured zinc oxide film for urea sensor," *Mater. Lett.* **63**, 2473–2475 (2009).
16. S. Saha et al., "Zinc oxide-potassium ferricyanide composite thin film matrix for biosensing applications," *Anal. Chim. Acta* **653**, 212–216 (2009).
17. A. Paliwal, M. Tomar, and V. Gupta, "Complex dielectric constant of various biomolecules as a function of wavelength using surface plasmon resonance," *J. Appl. Phys.* **116**, 023109 (2014).
18. A. Paliwal et al., "Optical properties of WO₃ thin films using surface plasmon resonance technique," *J. Appl. Phys.* **115**, 043104 (2014).
19. S. Saha et al., "Temperature dependent optical properties of (002) oriented ZnO thin film using surface plasmon resonance," *Appl. Phys. Lett.* **95**, 071106 (2009).
20. B. D. Cullity and S. R. Stock, *Elements of X-Ray Diffraction*, Prentice Hall, Inc., New Jersey (2001).
21. J. R. Sambles, G. W. Bradbery, and F. Yang, "Optical excitation of surface plasmons: an introduction," *Contemp. Phys.* **32**, 173–183 (1991).
22. S. K. Ozdemir and G. Turhan-Sayan, "Temperature effects on surface plasmon resonance: design considerations for an optical temperature sensor," *J. Lightwave Technol.* **21**, 805 (2003).
23. S. Shandilya et al., "Temperature dependent optical properties of c axis oriented LiNbO₃ thin film using surface plasmon resonance," *J. Lightwave Technol.* **28**(20), 3004–3011 (2010).
24. N. Batra et al., "Laser ablated ZnO thin film for amperometric detection of urea," *J. Appl. Phys.* **114**, 124702 (2013).
25. M. Tyagi, M. Tomar, and V. Gupta, "NiO nanoparticle-based urea biosensor," *Biosens. Bioelectron.* **41**, 110–115 (2013).
26. J. Homola, I. Koudela, and S. S. Yee, "Surface plasmon resonance sensors based on diffraction gratings and prism couplers: sensitivity comparison," *Sens. Actuators B* **54**(1–2), 16–24 (1999).
27. H. Raether, *Surface Plasmons on Smooth and Rough Surfaces and on Gratings*, Springer Verlag, Berlin Hiedelberg, Tokyo (1986).
28. K. D. Beyer and D. D. Ebeling, "UV refractive indices of aqueous ammonium sulfate solutions," *Geophys. Res. Lett.* **25**(16), 3147–3150 (1998).
29. R. Umaphathi, P. Attri, and P. Venkatesu, "Thermophysical properties of aqueous solution of ammonium-based ionic liquids," *J. Phys. Chem. B* **118**, 5971–5982 (2014).
30. R. Koncki, G. J. Mohr, and O. S. Wolfbeis, "Enzyme biosensor for urea based on a novel pH bulk optode membrane," *Biosens. Bioelectron.* **10**, 653–659 (1995).
31. A. A. Ansari, M. Azahar, and B. D. Malhotra, "Electrochemical urea biosensor based on sol-gel derived nanostructured cerium oxide," *J. Phys. Conf. Ser.* **358**, 012006 (2012).
32. N. Stasyuk et al., "Bi-enzyme L-arginine-selective amperometric biosensor based on ammonium-sensing polyaniline-modified electrode," *Biosens. Bioelectron.* **37**, 46–52 (2012).

Ayushi Paliwal received her BSc (2008) and MSc (2010) in physics from University of Delhi, Delhi, India. Presently, she is a senior research fellow (SRF) pursuing her PhD from the Department of Physics and Astrophysics, University of Delhi. Her research interests are in the development of optical sensors based on surface plasmon resonance technique for sensing toxic gases.

Monika Tomar received her BSc, MSc, and PhD degrees in physics in 1996, 1998, and 2005, respectively, from the University of Delhi. Presently, she is an assistant professor at Miranda House, University of Delhi, India. Her research interests include piezoelectric thin films for surface acoustics wave devices and sensors, oxide thin films, and nanostructures for gas sensing and biosensing applications, photonic devices, and so on.

Vinay Gupta received the BSc, MSc, and PhD degrees in physics in 1987, 1989, and 1995, respectively, from the University of Delhi, India. Presently, he is a professor in the Department of Physics and Astrophysics, University of Delhi. His current research interests are in piezoelectric thin films and layered structures, semiconductor and surface acoustic wave (SAW) sensors, ferroelectric films for electro-optic applications, and nanostructured oxide materials for multifunctional application.